

AN OPEN SOURCE TOOL FOR HEART RATE VARIABILITY WAVELET-BASED SPECTRAL ANALYSIS

Constantino A. García¹, Abraham Otero¹, Xosé Vila² and María J. Lado²

¹*Department of Software and Knowledge Engineering, University San Pablo CEU, 28668 Madrid, Spain*

²*Department of Computer Science, University of Vigo, Campus As Lagoas s/n, 32004 Ourense, Spain*

Keywords: Heart Rate Variability, Wavelet Transform, RHRV.

Abstract: Heart rate variability (HRV) power spectrum analysis is a well-known technique used to study the activity of the autonomic nervous system. It is performed by calculating the spectral power of certain bands of the RR time series. There are several tools that perform this type of analysis: Kubios HRV, PhysioNet's HRV toolkit for MatLab and aHRV, among others. All these tools use the Short Fourier Transform to estimate spectral power. However, the RR time series is a non-stationary signal. The Wavelet transform is often a more suitable tool for analyzing non-stationary signals than the Short Time Fourier Transform. Its usefulness in HRV analysis has already been proven in the literature. However, the lack of HRV analysis tools that support it has made this technique underutilized in HRV studies. In this paper we present an extension to the RHRV opensource package that enables Wavelet-based HRV spectral analysis. Until now this package only supported HRV spectral analysis based on the Fourier transform.

1 INTRODUCTION

Heart rate variability (HRV) analysis includes a set of techniques to study the beat-to-beat variations in the heart rate caused by the continuous modulation of the autonomic nervous system (ANS). One of the most powerful HRV techniques is based on the spectral analysis of a time series obtained from the distances between each pair of consecutive heartbeats. Relationships between the HRV spectral components and the different components of the ANS were experimentally demonstrated by Akselrod et al. (Akselrod et al., 1981), who described three relevant components in the HRV power spectrum: the very low frequency (VLF) component (frequencies below 0.03 Hz), which is modulated by the renina-angiotensin system; the low frequency (LF) component (0.03-0.15 Hz), which is thought to be of both sympathetic and parasympathetic nature; and the high frequency (HF) component (0.18-0.4 Hz), which is related to the parasympathetic system. At present, although authors agree on the existence of these three bands, there is no absolute consensus on the precise location of their boundaries.

The discrete Fourier transform is a common HRV spectral technique. It is a simple and fast technique, but its major disadvantage is its complete lack of tem-

poral resolution. This severely limits its capability to analyze a non-stationary signal, such as the RR time series. To alleviate this limitation the Short Time Fourier Transform (STFT) is often used in the HRV analysis. However, for solving this problem is often preferable to use the Wavelet transform, which provides control over both temporal and spectral (scale) resolution (Mallat, 1989).

The lack of tools for carrying out HRV analysis using the Wavelet transform has made this potentially superior analysis technique underutilized in the literature. HRV analysis tools such as Kubios HRV (Kubios, 2011), PhysioNet's HRV toolkit for MatLab (Matlab, 2011) or aHRV (Nevrokard-aHRV, 2011) only enable HRV spectral analysis based on the Fourier transform. Therefore, until now, the only option for performing HRV spectral analysis based on the Wavelet transform was to manually implement the analysis algorithms. In this paper we present an extension to the RHRV package (Rodríguez-Liñares et al., 2010) that enables Wavelet-based HRV spectral analysis. RHRV is an open source package for the R environment for statistical computing that comprises a complete set of tools for HRV analysis. Until now this package only supported HRV spectral analysis based on the Fourier transform.

The structure of this paper is as follows: first,

we shall briefly review the theory of Fast Orthogonal Wavelet Transform and we shall introduce one of its variants, the Maximum Overlap Discrete Wavelet Packet Transform (MODWPT). Next, we shall explain the algorithm used to compute the spectral power in the bands used in HRV analysis from the MODWPT scalogram. Fourier and Wavelet based analyses will be compared on simulated and real signals, and a discussion on the results of this paper will be provided.

2 MATERIAL AND METHODS

2.1 Multiresolution Analysis

The wavelet transform is a powerful tool for analyzing non-stationary signals, such as the RR time series. The analysis is based on the *mother wavelet*, a well-localized, oscillating, regular function $\psi(t)$. Mother wavelets functions, unlike the sinusoidal functions on which Fourier transform is based, are localized in space. This endows the Wavelet transform with both temporal and spectral (scale) resolution, which makes it preferable to the Fourier transform for the analysis of non stationary signals.

$\psi(t)$ can be considered as a band-pass filter that can be translated and dilated in time, yielding a set of wavelet functions:

$$\Psi_{u,s}(t) = \frac{1}{\sqrt{s}} \psi\left(\frac{t-u}{s}\right) \quad (1)$$

where $s > 0$ is a dilation factor, and u is a real number representing the translations.

The analysis of a function $f(t)$ using wavelets consists in the extraction of the signal information, and the synthesis permits the recovering of the original function from the representation obtained in the analysis. In both cases, the information is represented by several wavelet coefficients, which usually provide a redundant description of the original signal. However, for certain specific values of both the dilation and translation parameters, the wavelet functions constitute an orthonormal basis of $\mathbf{L}^2(\mathbb{R})$, and originate the *multiresolution analysis*.

The multiresolution analysis transforms a function in a successive set of decomposition levels in which each level increases the temporal resolution of the decomposition, at the expense of losing spectral resolution. The approximation of a function at a resolution 2^{-j} , $j \in \mathbb{Z}$, is defined as an orthogonal projection on a space $\mathbf{V}_j \subset \mathbf{L}^2(\mathbb{R})$, where the space \mathbf{V}_j contains all possible approximations at the resolution 2^{-j} . Let

$\{\mathbf{V}_j\}_{j \in \mathbb{Z}}$ be a multiresolution approximation verifying $V_{j+1} \subset \mathbf{V}_j \forall j \in \mathbb{Z}$ and let \mathbf{W}_j be the orthogonal complement of \mathbf{V}_j in V_{j-1} : $V_{j-1} = \mathbf{V}_j \oplus \mathbf{W}_j$. According to (Mallat, 1999), the families

$$\{\phi_{j,n} = \frac{1}{\sqrt{2^j}} \phi\left(\frac{t-2^j n}{2^j}\right)\}_{n \in \mathbb{Z}} \quad (2)$$

$$\{\psi_{j,n} = \frac{1}{\sqrt{2^j}} \psi\left(\frac{t-2^j n}{2^j}\right)\}_{n \in \mathbb{Z}} \quad (3)$$

are an orthonormal basis for \mathbf{V}_j and \mathbf{W}_j , respectively, for all $j \in \mathbb{Z}$. $\psi_{j,n}$ are the wavelet functions and $\phi_{j,n}$ are the scale functions. Thus, we can approximate any function $f \in \mathbf{L}^2(\mathbb{R})$ at the resolution 2^j as

$$P_{\mathbf{V}_j} f = \sum_{n=-\infty}^{\infty} \langle f, \phi_{j,n} \rangle \phi_{j,n} = \sum_{n=-\infty}^{\infty} a_j[n] \phi_{j,n} \quad (4)$$

and the orthogonal projection of f onto detail space \mathbf{W}_j is:

$$P_{\mathbf{W}_j} f = \sum_{n=-\infty}^{\infty} \langle f, \psi_{j,n} \rangle \psi_{j,n} = \sum_{n=-\infty}^{\infty} d_j[n] \psi_{j,n}. \quad (5)$$

where $a_j[n]$ and $d_j[n]$ are called the approximation and detail coefficients, respectively.

To compute approximation and detail coefficients, a filter bank can be used instead of the inner products. Let $h[n]$ and $g[n]$ be the FIR filters that will be used to compute the approximation and detail coefficients, respectively. It has been proven (Mallat, 1999) that $h[n] = \langle \phi_{j+1,0}, \phi_{j,n} \rangle$ and $g[n] = \langle \psi_{j+1,0}, \phi_{j,n} \rangle$. $g[n]$ filters can be regarded as an approximation to a high-pass filter, whereas $h[n]$ can be regarded as an approximation to a low-pass filter. Applying recursively over the approximation coefficients the same filtering operation followed by sub-sampling by two, we obtain the multiresolution expression of f . This algorithm, know as the pyramid algorithm, is the most efficient way of computing the Fast Orthogonal Wavelet Transform (FOWT).

Given that the FOWT can be reformulated in terms of filters, it can be used to calculate the spectral power in certain frequency bands. However, the FOWT only provides information on a limited set of frequency bands. To be able to calculate the spectral power in any given frequency band a slightly different transform needs to be used: the wavelet packet decomposition (WPD). In a WPD both detail and approximation coefficients (instead of only the approximation coefficients) are decomposed successively by applying high pass and low pass filters to each set of coefficients. Thus, the transform coefficients form a full binary tree.

Among the WPD transforms we have chosen the Maximal Overlap Discrete Wavelet Packet Transform (MODWPT) (Percival and Walden, 2006) because this transform avoids the sub-sampling step,

and therefore it has the same number of Wavelet coefficients in every decomposition level, and because it is well defined for non-dyadic sequences.

The j th level of the MODWPT decomposes the frequency interval $[0, f_s/2]$, where f_s is the sampling frequency of the original signal f , into 2^j equal width intervals. Each frequency interval will have N Wavelet coefficients associated, N being the length of the sampled signal f . The N -dimensional vector $\mathbf{W}_{j,n}$ will denote the N Wavelet coefficients associated with n th node (beginning at zero) in the j th level of the decomposition tree (see Figure 1). The n th node in the j th level of the decomposition tree, the (j, n) node, is associated with the frequency interval:

$$\frac{f_s}{2^{j+1}} [n, n+1] \quad (6)$$

The MODWPT coefficients fulfill that:

$$\|f\|^2 = \sum_{n=0}^{2^j-1} \|\mathbf{W}_{j,n}\|^2 \quad \forall j \quad (7)$$

Therefore, given a frequency band $[f_1, f_2] = \frac{f_s}{2^{j+1}} [k, k']$, being f_s the sampling frequency and k, k' and J integers, we can calculate the spectral power in $[f_1, f_2]$, $P([f_1, f_2])$, from the appropriate MODWPT coefficients. We just need to find the nodes (J, k) and (J, k') ; then we compute the spectral power in the band $[f_1, f_2]$ as:

$$P([f_1, f_2]) = \sum_{n=k}^{k'} \|\mathbf{W}_{J,n}\|^2 \quad (8)$$

2.2 Finding a Proper Cover

Equation 8 can only be applied to bands that can be written as $\frac{f_s}{2^{j+1}} [k, k']$, being f_s the sampling frequency and k, k' and J integers. In the general case, when performing a HRV spectral analysis the user may be interested in bands that cannot be written this way. This forces us to permit a certain error when we try to cover the bands specified by the user with coefficients obtained from the MODWPT decomposition (see Figure 2).

Let $[f_l, f_u]$ be the band in which we want to calculate the spectral power, and let ϵ_l, ϵ_u be the maximum errors allowed for the beginning and the ending of the band, respectively (RHRV allows the user to specify errors in absolute terms or relatively in % of the band's boundary value, but here we will work with absolute errors for the sake of simplicity). We need to find a node (j, n) whose lower frequency corresponds roughly to f_l with the tolerance allowed by ϵ_l ; that is:

$$f_l \in \frac{f_s}{2^{j+1}} [n, n+1], \quad (9)$$

$$f_l - \frac{f_s}{2^{j+1}} n \leq \epsilon_l. \quad (10)$$

Equation 9 allows us to perform a quick search of the adequate boundary node in the MODWPT decomposition tree, while Equation 10 defines a criterion of acceptability between the frequency values delimited by a node and the frequencies specified by the user. Analogously, we also need to find a node (j', n') whose upper frequency corresponds roughly to f_u with the tolerance allowed by ϵ_u :

$$f_u \in \frac{f_s}{2^{j'+1}} [n', n'+1], \quad (11)$$

$$\frac{f_s}{2^{j'+1}} (n'+1) - f_u \leq \epsilon_u. \quad (12)$$

The level j of the decomposition tree in which the node (j, n) that fulfills Equations 9 and 10 is found needs not be the same as the level j' in which the node (j', n') that fulfills Equations 11 and 12 is found. However, Equation 8 requires that $j = j'$. To avoid this problem, after the nodes (j, n) and (j', n') have been found, the node that is at the higher level is further decomposed to the level of the other node (see Figure 1). For example, let us suppose we have found the nodes (j, n) and (j', n') , $j < j'$, which correspond to the lower and upper limits of the frequency band, respectively. The lower frequency node (j, n) will be further decomposed $j' - j = m$ additional levels, obtaining as the new node corresponding to the lower limit of the band the node given by:

$$(j+m, n \cdot 2^m), \quad (13)$$

This situation is exemplified by the dotted nodes show in Figure 1. If the nodes (j, n) and (j', n') , are such that $j > j'$, the higher frequency node (j', n') will be further decomposed $j - j' = m$ additional levels, obtaining a new node that corresponds to the upper limit of the band. This node is given by:

$$(j+m, (n+1) \cdot 2^m - 1), \quad (14)$$

This situation is exemplified by the dashed nodes shown in Figure 1.

Figure 2 illustrates the complete search process for the band $[0.26, 0.99]$ Hz with $f_s = 2$ Hz and $\epsilon_u = \epsilon_l = 0.01$. We begin searching for the node whose lower limit corresponds to the frequency $f_l = 0.26$ Hz. The node $(1, 0)$ fulfills Equation 9, but not Equation 10. The node $(1, 1)$ neither fulfills Equation 9 nor Equation 10. Therefore, we continue the search decomposing the node $(1, 0)$ into the nodes $(2, 0)$ and $(2, 1)$. The node $(2, 0)$ does not verify Equation 9, but $(2, 1)$ verifies both Equation 9 and 10; i.e., $(2, 1)$ is the node whose lower limit corresponds to $f_l = 0.26$ Hz, with the tolerance indicated by ϵ_l . In Figure 2 the

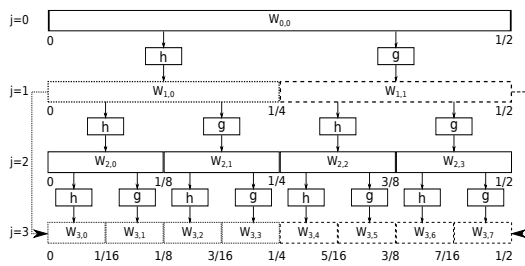


Figure 1: MODWPT decomposition tree showing an example of node relocation for lower (f_l) and upper (f_u) frequency nodes. $W_{0,0}$ represents the original signal, $f(t)$.

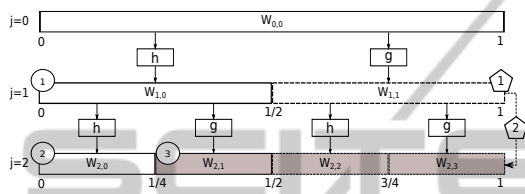


Figure 2: Search procedure for the nodes that cover the band $[0.26, 0.99]$ Hz.

search path for this node is shown with circles. We still have to find the node corresponding to the upper frequency $f_u = 0.99\text{Hz}$. For this frequency, (1, 1) verifies equations 11 and 12. Therefore our search ends. In Figure 2 the search path for this node is represented with the pentagon number 1.

However, the nodes corresponding with f_l and f_u are at different levels of the decomposition tree: levels 2 and 1, respectively. Before we can apply Equation 14, the node corresponding with f_u , (1, 1), must be further decomposed until it reaches level 2 of the tree, where the node corresponding with f_l , (2, 1), is located. In Figure 2 the relocation is represented by pentagon number 2. Finally, the power of the band can be computed as $P([0.26, 0.99]) \approx \sum_{n=1}^3 \|W_{2,n}\|^2$.

3 SOFTWARE DESCRIPTION

A more detailed description on how the open source RHRV package works can be found in (Rodríguez-Liñares et al., 2010). Here we will focus the description on the new functionality related to the extension presented in this article.

Listing 4 shows a basic example of RHRV using Wavelet analysis. `CreateHRVData()` creates a custom data structure to store all information related to the RR series and HRV analysis. `LoadBeatAscii()` loads beat positions stored in the ASCII file “BeatPosition.beats”. WFDB (Moody and Mark, 1990) data files can also be read with the function

`LoadBeatWFDB()`. Next, the function `BuildNIHR()` computes the instantaneous heart rate (the inverse of the time separation between two consecutive heart beats). Outliers and points with unacceptable physiological values can be removed using `FilterNIHR()`. An evenly spaced heart rate series is obtained with the `InterpolateNIHR()` function.

The function `CalculatePowerBand()` calculates the spectrogram and the power in the ULF, VLF, LF and HF spectral bands. Although the package provides default values for the boundaries of these bands, they can be overridden by the user. Default bands are ULF: $[0, 0.03]$ Hz, VLF: $[0.03, 0.05]$ Hz, LF: $[0.05, 0.15]$ Hz, HF: $[0.15, 0.4]$ Hz. Until now, this analysis could only be done using Short Time Fourier Transform (size and shift of the analysis window can be modified by the user). The algorithms presented in this paper were integrated into the `CalculatePowerBand()` function, allowing both Fourier and Wavelet analysis to be chosen by specifying an additional parameter. The default value for this parameter is “fourier”. The function has been modified in such a way that it is backwards compatible. Former code using the RHRV package will keep exactly the same behavior in the new version of the package.

When Wavelet analysis is selected in the `CalculatePowerBand()` function, the mother wavelet to be used in the analysis, the limits of the ULF, VLF, LF and HF bands and the error for each of the band boundaries can be specified by the user. The most used mother wavelets are available: Haar (“haar”), Daubechies (“d4”, “d6”, “d8” and “d16”) and the least asymmetric (“la8”, “la16” and “la20”), among others. The default mother wavelet is “d4” (Daubechies, 2006). When Wavelet analysis is used in the `CalculatePowerBand()` function, a tolerance for the bands’ boundaries is required for the power spectrum calculations. This tolerance is specified with the parameter `bandtolerance`, which takes a default value of 0.01.

4 RESULTS

In order to show how (at least in certain scenarios) the HRV analysis based on the Wavelet transform provides more temporal resolution than the Fourier transform, we will use a simulated RR series containing a sharp transition in its spectral components. The Integral Pulse Frequency Modulation (IPFM) model (Hyndman and Mohn, 1973) has been suggested as a functional description of the sino-atrial node. IPFM models how the pacemaker heart cells collect electric charge until the stored charge reaches a certain thresh-

Listing 1: Wavelet-based analysis in RHRV.

```
md = CreateHRVData( )
md = LoadBeatAscii(md, "BeatPositions.beats")
md = BuildNIHR(md)
md = FilterNIHR(md)
md = InterpolateNIHR(md, freqhr = 4)
md = CreateFreqAnalysis(md)
md = CalculatePowerBand(md, indexFreqAnalysis←
=1, ULFmin = 0, ULFmax=0.03, VLFmin = ←
0.03,VLFmax = 0.05, LFmin = 0.05, LFmax =←
0.15, HFmin= 0.15, nHFmax =0.4, type="←
wavelet", wavelet="d4", bandtolerance←
=0.01)
PlotPowerBand (md, indexFreqAnalysis=1)
```

old. Then the heartbeat is triggered.

Using the IPFM model we simulated an RR time series such as it only has spectral power in 0.03125 Hz from $t = 600 s$ to $t = 1200 s$; in 0.09375 Hz from $t = 1200 s$ to $t = 2400 s$; in 0.15625 Hz from $t = 2400 s$ to $t = 3600 s$. There it should present sharp transitions in the spectral components. We analyzed the spectrum of the resulting RR series with RHRV using Fourier (see Figure 3) and Wavelet (see Figure 4) transforms. Frequency bands for both analysis were VLF: [0,0.0625], .LF: [0.0625,0.125] HF: [0.125,0.5]. The mother Wavelet used in the analysis was Daubechies 4. Fourier analysis used a 30-second window with 12-second shift.

In Figures 3 and 4 red vertical lines delimit each of the three zones with different spectral components imposed by $m(t)$. It can be seen that wavelet analysis presents better time resolution than Fourier analysis. For each of the three spectral bands, and for each of the three zones with different spectral components, we calculated the ratio of the power that the band presents in each zone divided by the overall power of the band in the three zones. Theoretically, all the power in the VLF band should be in the first zone, all the power in the LF band should be in the second zone, and all the power in the HF band should be in the third zone. Therefore, the ideal ratios if perfect frequency discrimination is obtained are (1, 0, 0), (0, 1, 0) and (0, 0, 1). Tables 1 and 2 show the real ratios for Fourier and Wavelet analysis, respectively. It can be appreciated how Fourier has better frequency discrimination than Wavelets.

Finally, we analyzed the spectral components of an ECG recording of an obese 54-year old male who suffers from sleep apnea-hypopnea syndrome. The ECG recording was performed during a sleep test. The recording was analyzed using RHRV with the mother Wavelet Haar and with a tolerance in the band location of 0.01. Visual inspection of the results clearly shows that the spectral power in the band

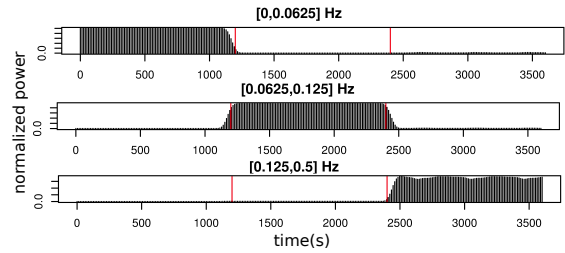


Figure 3: Fourier HRV analysis of the simulated RR series.

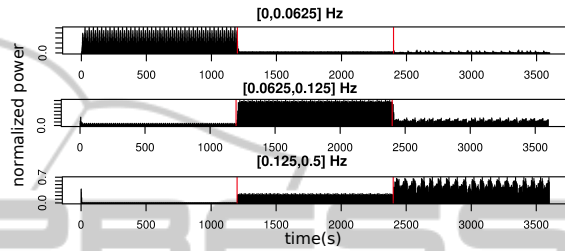


Figure 4: Wavelet HRV analysis of the simulated RR series.

Table 1: Relative power for Fourier analysis.

| | [0,1200] | [1200,2400] | [2400,3600] |
|-----|----------|-------------|-------------|
| ULF | 0,9785 | 0,0062 | 0,0153 |
| VLF | 0,0215 | 0,9317 | 0,0468 |
| LF | 0,0003 | 0,0030 | 0,9967 |

Table 2: Relative power for Wavelet analysis.

| | [0,1200] | [1200,2400] | [2400,3600] |
|-----|----------|-------------|-------------|
| ULF | 0,9309 | 0,0456 | 0,0235 |
| VLF | 0,0674 | 0,7695 | 0,1631 |
| LF | 0,0087 | 0,3057 | 0,6856 |

[0.125, 0.250] is higher during episodes of apnea and lower during normal breathing (see Figure 5). It should be noted that the higher power regions are remarkably well localized in time. We tried to replicate these results using Fourier, but we fail due to its lower temporal resolution.

5 DISCUSSION AND CONCLUSIONS

This paper presents what we believe to be the first HRV analysis toolkit that supports Wavelet-based spectral analysis of the RR time series. To perform such analysis the user only has to specify the spectral bands to be analyzed and, optionally, a tolerance for the position of the bands' boundaries (default tolerance is 0.01) and a mother Wavelet to be used in the analysis (by default is "db4"). This functionality has

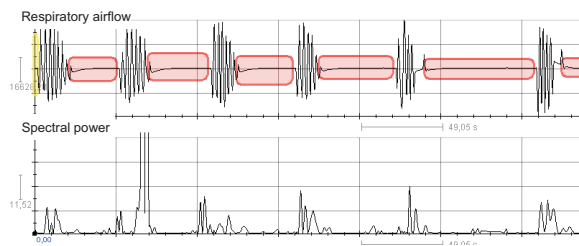


Figure 5: Spectral power in the band $[0.125, 0.250]$ is higher during apnea episodes than during normal breathing.

been implemented as an extension to the open source R package RHRV. The API of the new version of the package is fully backwards compatible.

The results presented here suggest that Wavelet-based analysis has a higher temporal resolution than Fourier-based analysis. On the other hand, Fourier is able to discriminate more precisely the spectral components present in the signal. The results presented in this paper are consistent with other similar tests conducted by the authors.

However, it should be noted that as we descend to lower levels in the frequency decomposition tree when looking for a suitable node cover for a frequency band, frequency resolution increases and temporal resolution decreases because of the Gabor-Heisenberg uncertainty principle for signals: $(\Delta t \Delta f \geq 1/2)$ (Gabor, 1953). To obtain optimal temporal resolution, we should avoid descending to deep levels of the tree. Our initial tests suggest that no more than five or six levels of the frequency decomposition tree should be expanded. In this sense, a careful selection of the frequency bands to be analyzed provides some control over the depth of the tree.

A corollary of the phenomenon described in the previous paragraph is that in order to achieve optimal temporal resolution the spectral bands used in HRV analysis with Wavelets will probably have to differ from those traditionally associated with ULF, VLF, LF and HF. This opens the question of what may be the pathophysiological significance of spectral bands different from those which have already been widely studied in the literature.

The mother Wavelet used in analysis also influences frequency-time resolution because it determines the filter shape. Further study on how the mother Wavelet influences the results of the analysis is required to understand more precisely the tradeoffs of using Wavelets versus Fourier. For example, our initial tests suggest that Haar Wavelet has greater time resolution than Daubechies 4 Wavelet for HRV analysis, whereas the latter has a better filtering behaviour than the first one.

ACKNOWLEDGEMENTS

This work was partially supported by the Spanish MEC and the European FEDER under the grant TIN2009-14372-C03-03, and by the Xunta de Galicia under the grant PGIDIT06SIN30501PR.

REFERENCES

- Akselrod, S., Gordon, D., Ubel, F., Shannon, D., Berger, A., and Cohen, R. (1981). Power spectrum analysis of heart rate fluctuation: a quantitative probe of beat-to-beat cardiovascular control. *Science*, 213(4504):220.
- Daubechies, I. (2006). *Ten lectures on wavelets*. Society for industrial and applied mathematics.
- Gabor, D. (1953). Communication theory and physics. *Information Theory, IRE Professional Group on*, 1(1):48–59.
- Hyndman, B. and Mohn, R. (1973). A pulse modulator model for pacemaker activity. In *Digest of the 10th Int. Conf. Med. & Biol. Eng.*, page 223.
- Kubios (2011). <http://kubios.uku.fi>.
- Mallat, S. (1989). A theory for multiresolution signal decomposition: The wavelet representation. *Pattern Analysis and Machine Intelligence, IEEE Transactions on*, 11(7):674–693.
- Mallat, S. (1999). *A wavelet tour of signal processing. Second Edition*. Academic Pr.
- Matlab (2011). <http://www.mathworks.com/index.html>.
- Moody, G. and Mark, R. (1990). The MIT-BIH arrhythmia database on cd-rom and software for use with it. In *Computers in Cardiology*, pages 185–188.
- Nevrokard-aHRV (2011). <http://www.nevrokard.eu>.
- Percival, D. and Walden, A. (2006). *Wavelet methods for time series analysis*, volume 4. Cambridge Univ Pr.
- Rodríguez-Liñares, L., Méndez, A., Lado, M., Olivieri, D., Vila, X., and Gómez-Conde, I. (2010). An open source tool for heart rate variability spectral analysis. *Computer Methods and Programs in Biomedicine*.